ChemPubSoc Europe

DOI: 10.1002/cphc.201900219

CHEMPHYSCHEM Communications

A Trigonal Prismatic Cobalt(II) Complex as a Single Molecule Magnet with a Reduced Contribution from Quantum Tunneling

Alexander A. Pavlov,[a] Dmitry Y. Aleshin,[a, b] Svetlana A. Savkina,[a] Alexander S. Belov,[a] Nikolay N. Efimov,[c] Joscha Nehrkorn,[d, e] Mykhaylo Ozerov,[d] Yan Z. Voloshin,[a, c] Yulia V. Nelyubina,[a, c] and Valentin V. Novikov*[a]

Herein, we report a new trigonal prismatic cobalt(II) complex that behaves as a single molecule magnet. The obtained zero-field splitting, which is also directly accessed by THz-EPR spectroscopy ($-102.5\ cm^{-1}$), results in a large magnetization reversal barrier U of $205\ cm^{-1}$. Its effective value, however, is much lower ($101\ cm^{-1}$), even though there is practically no contribution from quantum tunneling to magnetization relaxation.

Since the discovery in 1993,[1] single molecule magnets (SMMs) attracted attention of both synthetic and material chemists owing to their individual molecules behaving as permanent magnets.[2–10] An SMM, after it has been magnetized in an applied magnetic field, keeps its magnetization over time as a result of the magnetization reversal energy barrier U between the states with $M_S = +S$ and $M_S = -S$. The higher this barrier, the longer the magnetization is kept if the Orbach 'over-the-barrier' relaxation mechanism prevails.

Magnetometry in alternating current magnetic fields (*ac*-magnetometry) is the most popular method in SMM research, which directly accesses the magnetization relaxation time; other techniques of choice are dc-magnetometry,[8,9] far-infrared spectroscopy,[11] magnetic circular dichroism,[12] NMR spectroscopy,[13–20] and electron paramagnetic resonance (EPR) spectroscopy.[21,22] The latter is rarely used for studying SMMs. At conventional frequencies, they are almost always EPR-silent, as the transition $M_S = -S \leftrightarrow +S$ is forbidden by the selection rules for large S, and high-lying $M_S = \pm 1/2$ Kramer's doublet is unpopulated. At extremely high frequencies, however, THz-EPR spectroscopy can access the inter-Kramer's transition $M_S = \pm S \leftrightarrow \pm(S-1)$ and therefore directly measure the ZFS value,[23–28] which is the key characteristic of an SMM related to the energy U of the magnetization reversal barrier $U = 2|D|$ with D being a zero-field splitting energy.

Many SMMs have been found since 1993[1] among the compounds both of lanthanides[29–33] and of transition metals.[34–37] For transition metal complexes, the largest magnetization reversal barrier was observed for linear two-coordinated high-spin (HS) complexes of cobalt(II)[38,39] and iron(I),[35] which are extremely air-sensitive. Recently, a new family of highly stable SMMs has also been recognized, the trigonal prismatic complexes[13,14,40,41] with the HS cobalt(II) ion fully incapsulated by a three dimensional cage ligand. Another member of this family, a cobalt(II) acetylmethylimidazole-oximate clathrochelate, is reported here to behave as an SMM according to THz-EPR spectroscopy, *ac*- and *dc*-magnetometry, CASSCF calculations and NMR spectroscopy.

The cobalt(II) clathrochelate **1** and its diamagnetic analogue **1 a**, the isostructural complex of zinc(II) (Figure S1), were easily obtained (Scheme 1) in boiling ethanol by the template condensation of 1-(1-methyl-1H-imidazol-2-yl)ethanone oxime with phenylboronic acid on the corresponding metal ion as a matrix, as previously described for 2-acetylpyridineoximate clathrochelates.[19]

The obtained cobalt(II) complex **1** shows a rather large ZFS value determined by THz-EPR spectroscopy. In the magnetic

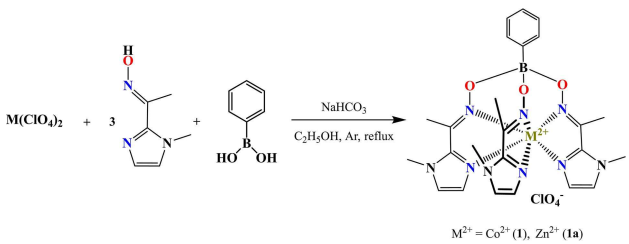

Scheme 1. Synthesis of cobalt(II) and zinc(II) acetylmethylimidazole-oximate clathrochelates **1** and **1 a**.

[a] Dr. A. A. Pavlov, D. Y. Aleshin, S. A. Savkina, A. S. Belov, Prof. Dr. Y. Z. Voloshin, Prof. Dr. Y. V. Nelyubina, Prof. Dr. V. V. Novikov
A. N. Nesmeyanov Institute of Organoelement Compounds
Russian Academy of Sciences
Vavilova str. 28, 119991, Moscow, Russia
E-mail: novikov84@ineos.ac.ru
[b] D. Y. Aleshin
D. Mendeleyev University of Chemical Technology of Russia
Miusskaya pl. 9, 125047, Moscow, Russia
[c] Dr. N. N. Efimov, Prof. Dr. Y. Z. Voloshin, Prof. Dr. Y. V. Nelyubina
Kurnakov Institute of General and Inorganic Chemistry
Russian Academy of Sciences
Leninskii prosp., 31, 117901, Moscow, Russia
[d] Dr. J. Nehrkorn, Dr. M. Ozerov
National High Magnetic Field Laboratory & Florida State University
1800 E. Paul Dirac Drive Tallahassee, FL 32310-3706, USA
[e] Dr. J. Nehrkorn
Max Planck Institute for Chemical Energy Conversion
Stiftstr. 34–36, 45470 Mülheim an der Ruhr, Germany

Supporting information for this article is available on the WWW under https://doi.org/10.1002/cphc.201900219

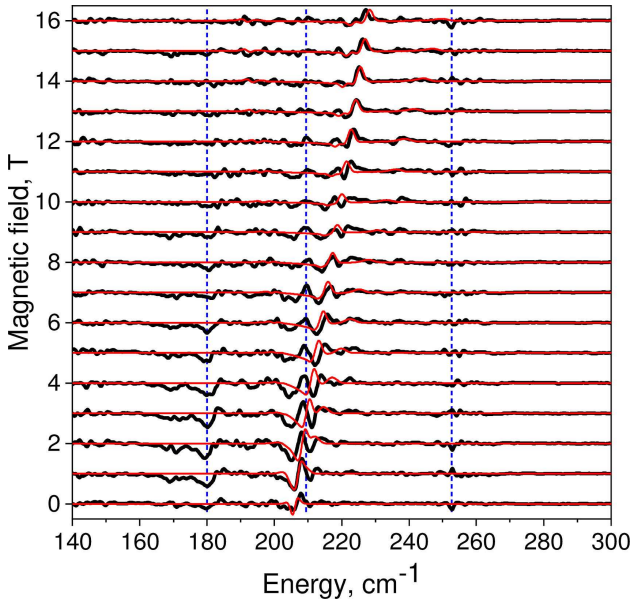

Figure 1. FD-FT THz-EPR MDS spectra of **1**. Experimental spectra and their simulations are shown as black and red lines, respectively. Data is rescaled and offset for the used magnetic field B_0. The dashed blue lines mark strong distortions of the spectra, which do not shift with magnetic field.

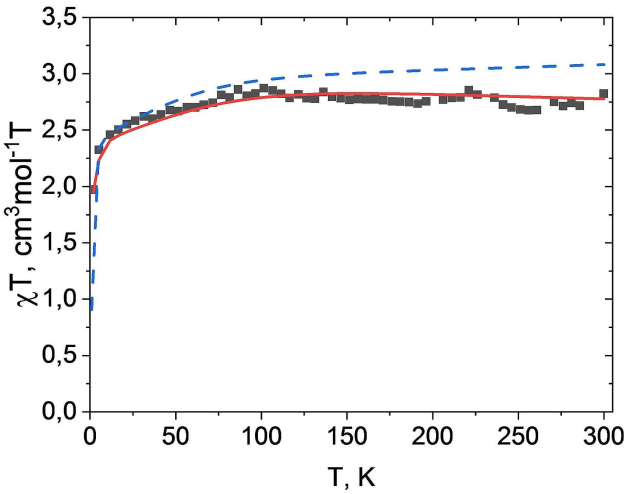

Figure 2. Variable temperature magnetic susceptibility data for a micro-crystalline sample of **1** collected under an applied dc-field of 5 kOe (dots). Red solid line shows fit to the data using Equation (1), blue dashed line represents the data from CASSCF calculation (see SI for more details).

field division spectra (MDS),[42] obtained by dividing a spectrum measured at B_0 by a spectrum measured at B_0+1 T, a maximum at 206 cm^{-1} is observed in the zero magnetic field (Figure 1), and a corresponding minimum at a lower energy is broad and shallow. Note that the region around 200 cm^{-1} in the spectra is particularly prone to distortions, which are mainly associated with the effects of magnetic field on the bolometric element. These distortions appear at different energies and with different intensities, but their positions are virtually independent of an applied magnetic field B_0. The observed magnetic feature at 206 cm^{-1} overlaps with one of such distortions, so its field-dependence is hard to follow at intermediate magnetic fields. However, it clearly shifts to higher energies upon increasing the magnetic field, allowing for its assignment as the ZFS with $|D| = 103$ cm^{-1}. Although the sign of the ZFS for a system with spin $S=3/2$ cannot be obtained by FD-FT THz-EPR, the complex **1** is EPR-silent at temperatures down to 5 K and at frequencies up to 320 GHz (10.7 cm^{-1}), indicating a negative ZFS value.

Molar magnetic susceptibility measured for a fine crystalline sample of **1** at 2–300 K by dc-magnetometry confirms the HS state of the cobalt(II) ion in this complex over the temperature range (Figure 2). At the room temperature, the measured χT value (2.85 $cm^3 mol^{-1} K$) is larger than the theoretical value for the HS cobalt(II) ion in the ground state without the spin-orbit coupling (SOC) (1.88 $cm^3 mol^{-1} K$), which is a signature of not fully quenched orbital moment; a decrease in the χT value upon cooling agrees with the ZFS effects.[34] A slight magnetic hysteresis loop observed at temperature of 2 K (Figure S3) also points to the SMM nature of **1**. Fitting the temperature-dependence of χT and the field-dependence of magnetization with the spin-Hamiltonian [Eq. (1)] using the ZFS value D equal to −102.5 cm^{-1}, as obtained by the THz-EPR spectroscopy, leads to the following parameters: $g_{\perp}=2.00$, $g_{||}=2.96$ (Figure 2). No good fit can be obtained with the positive value of ZFS, and accounting for the rhombicity also does not lead to a better convergence.

$$\hat{H} = D\left(\hat{S}_z^2 - \frac{S(S+1)}{3}\right) + g\mu_B B\hat{S} \quad (1)$$

Simulations of FD-FT THz-EPR MDS spectra by using the above g-factors reproduce the magnetic feature observed in these spectra (see Figure 1). Similar magnetic parameters are obtained from CASSCF/NEVPT2 calculations of the isolated complex **1** (see SI for details): $g_x=2.03$, $g_y=2.04$, $g_z=2.97$, $D=-82.7$ cm^{-1}, $E/D=0.007$.

The dc-magnetometry measures only the isotropic value of magnetic susceptibility tensor (**χ**) in the case of a fine-crystalline sample, while the anisotropy of this tensor Δχ can be estimated by variable-temperature liquid-state NMR spectroscopy for a paramagnetic compound. In the ^{1}H NMR spectrum of the cobalt (II) complex **1**, large chemical shifts at 235–345 K agree with its HS state and its molecular geometry with a C_3 pseudo-axis passing through the cobalt and boron atoms (Figures S8–S9). In this (axial) case, pseudo-contact contribution to the chemical shifts that arises from the magnetic anisotropy is described by Equation (2) (the diamagnetic contributions are taken as chemical shifts in the ^{1}H NMR spectra for the diamagnetic complex **1a**):

$$\delta_{PC} = \frac{1}{12\pi r^3}[\Delta\chi_{ax}(3\cos^2\theta - 1)] \quad (2)$$

By using the chemical shifts of the protons of the phenyl group as the δ_{PC} values, as those protons are too far from a paramagnetic metal ion to have a non-negligible contact

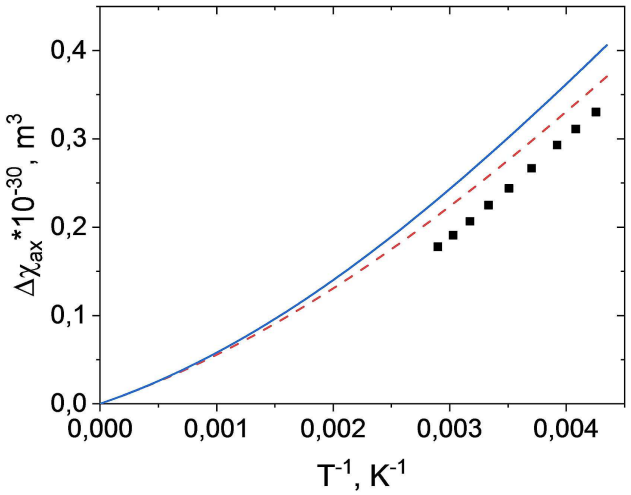

Figure 3. Temperature dependence of NMR-derived axial magnetic susceptibility tensor anisotropy for acetonitrile solution of **1** (dots). Red solid line shows the data from CASSCF calculation, blue dashed line represents the data from magnetic parameters obtained by fitting of THz-EPR and dc-magnetometry data.

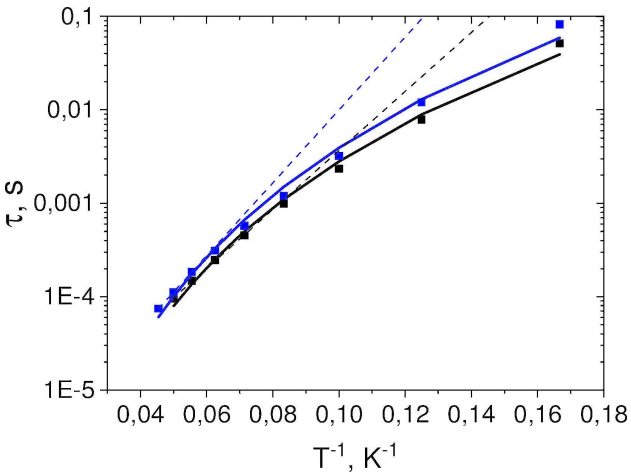

Figure 4. Temperature-dependence of the magnetization relaxation time τ under an applied magnetic field (blue) and in its absence (black). The solid lines represent the fit with the Equation (3), and the dashed lines are the linear fits by the Arrhenius expression $\tau = \tau_0 \exp(U_{eff}/kT)$; simulation parameters are collected in Table S2.

contribution from direct spin delocalization (Figure 3), we obtained an estimate for temperature dependence of the magnetic susceptibility tensor anisotropy $\Delta\chi_{ax}$. The chemical shifts of all other nuclei in the ^{1}H NMR spectra at 300 K agree well with obtained value of $\Delta\chi_{ax}$ at this temperature ($22.5 \cdot 10^{-32}$ m^3 at 300 K, Figure S10), which is rather large in comparison with the most other six-coordinated cobalt(II) complexes.[43]

The variation of $\Delta\chi_{ax}$ values obtained at different temperatures allows one to make some insightful conclusions on the ZFS value. If the magnetic anisotropy is small, the temperature dependence of $\Delta\chi_{ax}$ obeys the Curie law and is linear in the coordinates $\Delta\chi - T^{-1}$ and crosses the origin. If the magnetic anisotropy is large, it deviates from linearity. For the complex **1**, the observed non-Curie behavior of the $\Delta\chi_{ax}$ values suggests large ZFS caused by the unquenched orbital moment. Similar behavior is observed if the corresponding temperature dependence is extracted from the CASSCF calculation of the isolated complex **1** or from the THz-EPR and dc-magnetometry data for its fine crystalline sample (Figure 3). The latter methods, however, seem to overestimate the values of $\Delta\chi_{ax}$ as a result of crystal packing effects or, alternatively, the molecular mobility[44] such as a dynamic Jahn-Teller distortion.

The ZFS value obtained by all these techniques for the complex **1** should give rise to a large energy barrier U of magnetization reversal (205 cm^{-1} from THz-EPR spectroscopy). According to *ac*-magnetometry, however, the effective barriers U_{eff} are much lower (101 and 130 cm^{-1} in the zero-field and under an applied magnetic field). An observed nonlinear temperature-dependence of the magnetization relaxation time in Arrhenius coordinates $\ln(\tau) - T^{-1}$ indicates that relaxation mechanisms other than Orbach's operate in the system (Figure 4).

One of such 'non-Orbach' relaxation mechanisms that can completely quench slow magnetic relaxation is quantum tunneling. Reducing its efficiency is an established approach to increase the effective barrier to magnetization reversal,[45] which can be done by applying an external magnetic field. As it does not affect dramatically the relaxation time for the complex **1**, the quantum tunneling has a negligible contribution to the magnetization relaxation, as does the direct mechanism, in contrast to a previously published cobalt(II) tris-pyridineoximate clathrochelate[19] due to different crystal packing[4] or lower rhombicity[46] of **1**. At temperatures below 6 K, the relaxation times for **1** cannot be reliably obtained from the ac-magnetometry data, as the position of the maximum in frequency dependence of out-of-phase χ'' component of the magnetic susceptibility is at frequencies beyound the range of the magnetometer used (Figures S4, S5). These data, however, are clearly temperature-dependent, which is also a sign of the insignificant contribution from quantum tunneling. Therefore, the magnetization relaxation time for the complex **1** is dominated by Raman and Orbach mechanisms:

$$\tau^{-1} = \tau_0^{-1} \exp(-U/kT) + CT^n \quad (3)$$

where τ_0 is an attempt time, U is a magnetization reversal barrier, C is a coefficient, n is a variable parameter[47,48] usually equal to 9 for Kramers ions[49] but lower values may be expected if optical phonons are taken into account.[50,51]

The best fits to the temperature-dependence of the measured relaxation times for the complex **1** using Equation (3) reveal the total dominance of the Raman mechanism without Orbach impact (Figure 4). On the other hand, the significant deviations from an exponential Arrhenius dependence of an Orbach process can be observed for SMMs with large magnetic anisotropy ($U > kT$) due to spin–phonons coupling,[52] leading more complicated behavior of a relaxation time than described by eq. (3); therefore non-exponential Orbach-type process cannot be completely ruled out.

In conclusion the reported trigonal prismatic tris-imidazole-oximate cobalt(II) complex is a new SMM with the zero-field splitting directly measured by a very demanding THz-EPR spectroscopy ($-102.5\ cm^{-1}$) that results in a large magnetization reversal barrier of $205\ cm^{-1}$. Its effective value, however, is much lower ($101\ cm^{-1}$), as confirmed by ac- and dc-magnetometry, CASSCF calculations and widely available NMR spectroscopy. An important feature of this SMM is that there is practically no unwanted contribution from quantum tunneling to the magnetization relaxation, which is totally dominated by the Raman mechanism, in contrast to the previously published cobalt(II) tris-pyridineoximate analogue. The reasons behind it, such as different crystal packing or lower rhombicity, are now under investigation in our group.

Acknowledgements

This study was financially supported by Russian Science Foundation (project No. 17-73-20369). THz-EPR experiments were performed at the National High Magnetic Field Laboratory, which is supported by National Science Foundation Cooperative Agreement No. DMR-1644779 and the State of Florida. X-ray diffraction data were collected with the financial support from Ministry of Science and Higher Education of the Russian Federation using the equipment of Center for molecular composition studies of INEOS RAS. Magnetic measurements were performed using equipment of the JRC PMR IGIC RAS.

Conflict of interest

The authors declare no conflict of interest.

Keywords: cage compounds · high-spin cobalt(II) complexes · paramagnetic NMR spectroscopy · single molecule magnets · THz-EPR spectroscopy

[1] R. Sessoli, D. Gatteschi, A. Caneschi, M. Novak, *Nature.* **1993**, *365*, 141–143.
[2] R. Sessoli, A. K. Powell, *Coord. Chem. Rev.* **2009**, *253*, 2328–2341.
[3] J. M. Frost, K. L. Harriman, M. Murugesu, *Chem. Sci.* **2016**, *7*, 2470–2491.
[4] D. Gatteschi, R. Sessoli, *Angew. Chem. Int. Ed.* **2003**, *42*, 268–297; *Angew. Chem.* **2003**, *115*, 278–309.
[5] L. Bogani, *Nat. Mater.* **2008**, *7*, 179.
[6] R. E. Winpenny, *Angew. Chem. Int. Ed.* **2008**, *47*, 7992–7994; *Angew. Chem.* **2008**, *120*, 8112–8114.
[7] M. Atanasov, D. Aravena, E. Suturina, E. Bill, D. Maganas, F. Neese, *Coord. Chem. Rev.* **2015**, *289*, 177–214.
[8] D. N. Woodruff, R. E. Winpenny, R. A. Layfield, *Chem. Rev.* **2013**, *113*, 5110–5148.
[9] D. Gatteschi, R. Sessoli, J. Villain, Molecular nanomagnets, *Oxford University Press on Demand*, **2006**.
[10] S. G. McAdams, A.-M. Ariciu, A. K. Kostopoulos, J. P. Walsh, F. Tuna, *Coord. Chem. Rev.* **2017**, *346*, 216–239.
[11] R. Boča, *Coord. Chem. Rev.* **2004**, *248*, 757–815.
[12] M. Mannini, F. Pineider, C. Danieli, F. Totti, L. Sorace, P. Sainctavit, M.-A. Arrio, E. Otero, L. Joly, J. C. Cezar, *Nature.* **2010**, *468*, 417–421.
[13] V. V. Novikov, A. A. Pavlov, Y. V. Nelyubina, M.-E. Boulon, O. A. Varzatskii, Y. Z. Voloshin, R. E. Winpenny, *J. Am. Chem. Soc.* **2015**, *137*, 9792–9795.
[14] A. A. Pavlov, Y. V. Nelyubina, S. V. Kats, L. V. Penkova, N. N. Efimov, A. O. Dmitrienko, A. V. Vologzhanina, A. S. Belov, Y. Z. Voloshin, V. V. Novikov, *J. Phys. Chem. Lett.* **2016**, *7*, 4111–4116.
[15] M. Damjanović, P. P. Samuel, H. W. Roesky, M. Enders, *Dalton Trans.* **2017**, *46*, 5159–5169.
[16] M. Hiller, S. Krieg, N. Ishikawa, M. Enders, *Inorg. Chem.* **2017**, *56*, 15285–15294.
[17] T. Morita, M. Damjanović, K. Katoh, Y. Kitagawa, N. Yasuda, Y. Lan, W. Wernsdorfer, B. K. Breedlove, M. Enders, M. Yamashita, *J. Am. Chem. Soc.* **2018**, *140*, 2995–3007.
[18] M. Damjanovic, K. Katoh, M. Yamashita, M. Enders, *J. Am. Chem. Soc.* **2013**, *135*, 14349–14358.
[19] A. A. Pavlov, S. A. Savkina, A. S. Belov, Y. V. Nelyubina, N. N. Efimov, Y. Z. Voloshin, V. V. Novikov, *Inorg. Chem.* **2017**, *56*, 6943–6951.
[20] A. A. Pavlov, S. A. Savkina, A. S. Belov, Y. Z. Voloshin, Y. V. Nelyubina, V. V. Novikov, *ACS Omega.* **2018**, *3*, 4941–4946.
[21] M. L. Baker, S. J. Blundell, N. Domingo, S. Hill in *Spectroscopy methods for molecular nanomagnets, Vol.*, Springer, **2014**, pp.231–291.
[22] A. B. Boeer, D. Collison, E. J. McInnes *Electron Paramagn. Reson.* **2008**, *21*.
[23] J. Nehrkorn, S. L. Veber, L. A. Zhukas, V. V. Novikov, Y. V. Nelyubina, Y. Z. Voloshin, K. Holldack, S. Stoll, A. Schnegg, *Inorg. Chem.* **2018**, *57*, 15330–15340.
[24] E. A. Suturina, J. Nehrkorn, J. M. Zadrozny, J. Liu, M. Atanasov, T. Weyhermüller, D. Maganas, S. Hill, A. Schnegg, E. Bill, *Inorg. Chem.* **2017**, *56*, 3102–3118.
[25] J. Nehrkorn, J. Telser, K. Holldack, S. Stoll, A. Schnegg, *J. Phys. Chem. B.* **2015**, *119*, 13816–13824.
[26] J. Dreiser, A. Schnegg, K. Holldack, K. S. Pedersen, M. Schau-Magnussen, J. Nehrkorn, P. Tregenna-Piggott, H. Mutka, H. Weihe, J. Bendix, *Chem. Eur. J.* **2011**, *17*, 7492–7498.
[27] D. Pinkowicz, H. I. Southerland, C. Avendaño, A. Prosvirin, C. Sanders, W. Wernsdorfer, K. S. Pedersen, J. Dreiser, R. Clérac, J. Nehrkorn, *J. Am. Chem. Soc.* **2015**, *137*, 14406–14422.
[28] J. Lu, I. O. Ozel, C. A. Belvin, X. Li, G. Skorupskii, L. Sun, B. K. Ofori-Okai, M. Dincă, N. Gedik, K. A. Nelson, *Chem. Sci.* **2017**, *8*, 7312–7323.
[29] C. A. Goodwin, F. Ortu, D. Reta, N. F. Chilton, D. P. Mills, *Nature.* **2017**, *548*, 439–442.
[30] J. Liu, Y.-C. Chen, J.-L. Liu, V. Vieru, L. Ungur, J.-H. Jia, L. F. Chibotaru, Y. Lan, W. Wernsdorfer, S. Gao, *J. Am. Chem. Soc.* **2016**, *138*, 5441–5450.
[31] Y.-C. Chen, J.-L. Liu, L. Ungur, J. Liu, Q.-W. Li, L.-F. Wang, Z.-P. Ni, L. F. Chibotaru, X.-M. Chen, M.-L. Tong, *J. Am. Chem. Soc.* **2016**, *138*, 2829–2837.
[32] M. Gregson, N. F. Chilton, A.-M. Ariciu, F. Tuna, I. F. Crowe, W. Lewis, A. J. Blake, D. Collison, E. J. McInnes, R. E. Winpenny, *Chem. Sci.* **2016**, *7*, 155–165.
[33] S. T. Liddle, J. van Slageren, *Chem. Soc. Rev.* **2015**, *44*, 6655–6669.
[34] J. M. Zadrozny, M. Atanasov, A. M. Bryan, C.-Y. Lin, B. D. Rekken, P. P. Power, F. Neese, J. R. Long, *Chem. Sci.* **2013**, *4*, 125–138.
[35] J. M. Zadrozny, D. J. Xiao, M. Atanasov, G. J. Long, F. Grandjean, F. Neese, J. R. Long, *Nat. Chem.* **2013**, *5*, 577–581.
[36] D. E. Freedman, W. H. Harman, T. D. Harris, G. J. Long, C. J. Chang, J. R. Long, *J. Am. Chem. Soc.* **2010**, *132*, 1224–1225.
[37] Y. Rechkemmer, F. D. Breitgoff, M. Van Der Meer, M. Atanasov, M. Hakl, M. Orlita, P. Neugebauer, F. Neese, B. Sarkar, J. Van Slageren, *Nat. Commun.* **2016**, *7*, 10467.
[38] P. C. Bunting, M. Atanasov, E. Damgaard-Møller, M. Perfetti, I. Crassee, M. Orlita, J. Overgaard, J. van Slageren, F. Neese, J. R. Long, *Science.* **2018**, *362*, eaat7319.
[39] X.-N. Yao, J.-Z. Du, Y.-Q. Zhang, X.-B. Leng, M.-W. Yang, S.-D. Jiang, Z.-X. Wang, Z.-W. Ouyang, L. Deng, B.-W. Wang, *J. Am. Chem. Soc.* **2016**, *139*, 373–380.
[40] B. Yao, Y.-F. Deng, T. Li, J. Xiong, B.-W. Wang, Z. Zheng, Y.-Z. Zhang, *Inorg. Chem.* **2018**, *57*, 14047–14051.
[41] T. J. Ozumerzifon, I. Bhowmick, W. C. Spaller, A. K. Rappé, M. P. Shores, *Chem. Commun.* **2017**, *53*, 4211–4214.
[42] J. Nehrkorn, K. Holldack, R. Bittl, A. Schnegg, *J. Magn. Reson.* **2017**, *280*, 10–19.
[43] I. Bertini, C. Luchinat, G. Parigi, R. Pierattelli, *ChemBioChem.* **2005**, *6*, 1536–1549.
[44] D. Shishmarev, G. Otting, *J. Biomol. NMR.* **2013**, *56*, 203–216.
[45] S. Hill, S. Datta, J. Liu, R. Inglis, C. J. Milios, P. L. Feng, J. J. Henderson, E. del Barco, E. K. Brechin, D. N. Hendrickson, *Dalton Trans.* **2010**, *39*, 4693–4707.

[46] M. Atanasov, J. M. Zadrozny, J. R. Long, F. Neese *Chem. Sci.* **2013**, *4*, 139–156.
[47] M. A. Palacios, J. Nehrkorn, E. A. Suturina, E. Ruiz, S. Gomez-Coca, K. Holldack, A. Schnegg, J. Krzystek, J. M. Moreno, E. Colacio, *Chem. Eur. J.* **2017**, *23*, 11649–11661.
[48] F. Liu, D. S. Krylov, L. Spree, S. M. Avdoshenko, N. A. Samoylova, M. Rosenkranz, A. Kostanyan, T. Greber, A. U. Wolter, B. Büchner *Nat. Commun.* **2017**, *8*, 16098.
[49] A. Abragam, B. Bleaney, *Electron paramagnetic resonance of transition ions*, OUP Oxford, **2012**.
[50] K. Shrivastava, *Phys. Status Solidi B.* **1983**, *117*, 437–458.
[51] E. Colacio, J. Ruiz, E. Ruiz, E. Cremades, J. Krzystek, S. Carretta, J. Cano, T. Guidi, W. Wernsdorfer, E. K. Brechin, *Angew. Chem. Int. Ed.* **2013**, *52*, 9130–9134; *Angew. Chem.* **2013**, *125*, 9300–9304.
[52] A. Lunghi, F. Totti, R. Sessoli, S. Sanvito, *Nat. Commun.* **2017**, *8*, 14620.

Manuscript received: March 5, 2019
Version of record online: April 5, 2019